

# Computational Modelling of Isotropic Multiplicative Growth

G. Himpel, E. Kuhl, A. Menzel, P. Steinmann<sup>1</sup>

**Abstract:** The changing mass of biomaterials can either be modelled at the constitutive level or at the kinematic level. This contribution attends on the description of growth at the kinematic level. The deformation gradient will be multiplicatively split into a growth part and an elastic part. Hence, in addition to the material and the spatial configuration, we consider an intermediate configuration or grown configuration without any elastic deformations. With such an ansatz at hand, contrary to the modelling of mass changes at the constitutive level, both a change in density and a change in volume can be modelled.

The algorithmic realisation of this framework within a finite element setting constitutes the main contribution of this paper. To this end the key kinematic variable, i.e. the isotropic stretch ratio, is introduced as internal variable at the integration point level. The consistent linearisation of the stress update based on an implicit time integration scheme is developed. Basic features of the model are illustrated by means of representative numerical examples.

**keyword:** Biomaterials, growth, remodelling, multiplicative decomposition

## 1 Introduction

The modelling of biomaterials with changing mass can be classified in terms of two different approaches, the coupling of mass changes and deformations at the constitutive level and the coupling at the kinematic level, whereby both theories can be combined in one framework.

A changing mass at the constitutive level is typically realised by a weighting of the free energy function with respect to the density field. Such an ansatz enables the simulation of changes in density while the overall vol-

ume remains unaffected by growth. We will call this effect ‘remodelling’. Although in principle applicable for small and large strains, this approach is typically adopted for hard tissues, which usually undergo small strain deformations. The first continuum model in this regard has been advocated by Cowin & Hegedus (1976). In the last decades this model which is embedded into the thermodynamics of open systems has been elaborated further by, for instance, Harrigan & Hamilton (1992; 1993), Epstein & Maugin (2000), Kuhl et al. (2003), Kuhl & Steinmann (2003a; 2004), Himpel (2003) and Menzel (2005; 2005a).

Within the kinematic coupling, a changing mass is characterised through a multiplicative decomposition of the deformation gradient into a growth part and an elastic part, as first introduced in the context of plasticity by Lee (1969). In this formulation, which we will refer to as ‘growth’ in the sequel, mass changes are attributed to changes in volume while the material density remains constant. This approach has classically been applied to model soft tissues undergoing large strains. The first contribution including this ansatz is the work by Rodriguez et al. (1994). Further elaborations can be found in the publications by Taber & Perucchio (2000), Chen & Hoger (2000), Klisch et al. (2001), Ambrosi & Mollica (2002), Imatani & Maugin (2002), Humphrey (2002), Humphrey & Delange (2004), Humphrey & Rajagopal (2002), Rao et al. (2003), Garikipati et al. (2004) and Menzel (2005a). The present paper is essentially based on the recent work of Lubarda & Hoger (2002) which combines both, growth and remodelling, i.e. changes in volume and changes in density. Naturally, the classical open system approach by Cowin & Hegedus (1976), introducing the change of mass at the constitutive level, and the ansatz of Rodriguez et al. (1994), introducing a coupling of mass changes and deformations at the kinematic level, are included as special cases. As a main contribution of this work, we will discuss the algorithmic setup of the advocated material model.

---

<sup>1</sup>Chair of Applied Mechanics, Department of Mechanical and Process Engineering, University of Kaiserslautern, Germany, <http://mechanik.mv.uni-kl.de>

The present paper is organised as follows: The growth remodelling framework is reviewed in section 2. This includes the introduction of the multiplicative split of the deformation gradient as well as the detailed description of the consequences of this split to the density expressions. Essential balance equations are presented before the model is specified to different cases for a mass change. The constitutive equations are presented in section 3. A free energy function and the evolution of the growth deformation gradient are suggested. These constitutive functions are then specified to the special cases of a pure density change and a pure volume change. In section 4 we concentrate on the numerical implementation of the constitutive framework for the density preserving approach. This includes the algorithmic treatment of the stretch ratio evolution as well as the computation of the incremental tangent modulus within a finite element setting. The theory will be discussed by means of numerical examples in section 5. We first drive a simple tension test to demonstrate the sensitivity with respect to the material parameters. Then the theory will be applied to a boundary value problem. Finally, the results of the paper are summarised in section 6.

## 2 Kinematics

In this section we discuss the kinematics of finite growth. For a general overview on the continuum mechanics of finite deformations the reader is referred to the monographs by Ogden (1997) and Holzapfel (2000). The basic quantities will be introduced and necessary correlations will be given. Essential balance equations are reviewed and finally we present three different forms in which a change of mass can occur. We consider the deformation map  $\boldsymbol{\varphi}$  of a material placement  $\mathbf{X}$  in the material configuration  $B_0$  at time  $t_0$  to the spatial placement  $\mathbf{x}$  in the spatial configuration  $B_t$  at time  $t$ . The corresponding deformation gradient  $\mathbf{F}$  denotes the tangent map from the material tangent space  $T_{\mathbf{X}}B_0$  to the spatial tangent space  $T_{\mathbf{x}}B_t$

$$\mathbf{F} = \nabla_{\mathbf{X}}\boldsymbol{\varphi}(\mathbf{X}, t) : T_{\mathbf{X}}B_0 \rightarrow T_{\mathbf{x}}B_t. \quad (1)$$

The related Jacobian is denoted by  $J = \det \mathbf{F} > 0$ . The cofactor of the deformation gradient  $\text{cof} \mathbf{F} = J\mathbf{F}^{-t}$  maps a material area element  $d\mathbf{A}$  to a spatial area element  $d\mathbf{a}$ . Since the Jacobian constitutes a scalar value,  $\mathbf{F}^{-t}$  denotes the normal map from the material cotangent space

$T_{\mathbf{X}}^*B_0$  to the spatial cotangent space  $T_{\mathbf{x}}^*B_t$

$$\mathbf{F}^{-t} : T_{\mathbf{X}}^*B_0 \rightarrow T_{\mathbf{x}}^*B_t. \quad (2)$$

Further on the metric tensors  $\mathbf{G}$  in the material configuration and  $\mathbf{g}$  in the spatial configuration are introduced, which relate the tangent and cotangent spaces. Therewith we define the right Cauchy-Green tensor

$$\mathbf{C} = \mathbf{F}^t \cdot \mathbf{g} \cdot \mathbf{F} \quad (3)$$

as a deformation measure in the material configuration. Its spatial counterpart is represented by the left Cauchy-Green tensor

$$\mathbf{b} = \mathbf{F} \cdot \mathbf{G}^{-1} \cdot \mathbf{F}^t. \quad (4)$$

The material time derivative of a material quantity  $\{\bullet\}$  will be denoted by  $\{\dot{\bullet}\} = \partial_t \{\bullet\}|_{\mathbf{X}}$ . The spatial velocity gradient can be introduced in the form

$$\mathbf{l} := \nabla_{\mathbf{x}}\mathbf{v} = \dot{\mathbf{F}} \cdot \mathbf{F}^{-1}, \quad (5)$$

with  $\mathbf{v} = \dot{\mathbf{x}}$  denoting the spatial velocity.

### 2.1 Multiplicative decomposition

The deformation of the body during the growth process can be decomposed into two parts. At first every particle of the body grows or alternatively decreases. This growth part of the deformation results in an intermediate configuration  $\widehat{B}_0$ , which does not necessarily has to be compatible. Hence an additional elastic deformation might be needed to ensure compatibility of the total deformation. This phenomenon is clearly illustrated in Rodriguez et al. (1994) considering a growing ventricle as example. According to this considerations we assume a multiplicative split of the deformation gradient

$$\mathbf{F} = \mathbf{F}_e \cdot \mathbf{F}_g \quad (6)$$

into a growth deformation gradient  $\mathbf{F}_g$  and a purely elastic deformation gradient  $\mathbf{F}_e$ . An illustration of this assumption is given in Fig. 1. In the theory of elastoplasticity an analogous split was first introduced by Lee (1969) and has been applied to several material models. A comparison of constitutive theories based on a multiplicative split of the deformation gradient is given in Lubarda (2004).

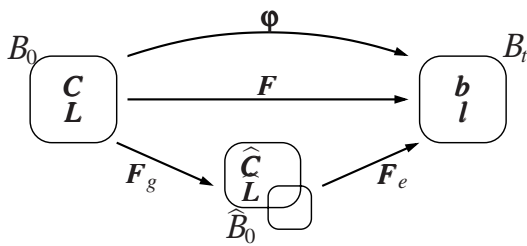


**Figure 1** : The total deformation gradient  $\mathbf{F}$  is multiplicative split into a growth part  $\mathbf{F}_g$  and an elastic part  $\mathbf{F}_e$ . The intermediate or grown state  $\hat{B}_0$  is incompatible.

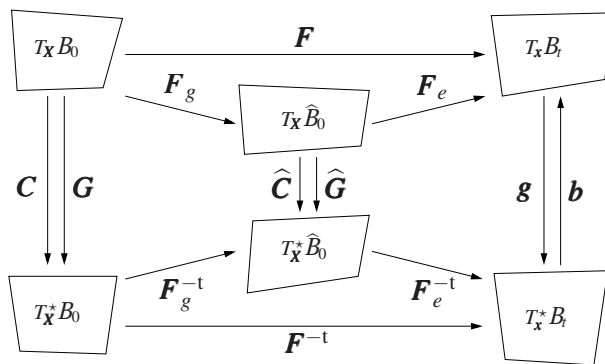


**Figure 2** : Visualisation of the metric tensors and the deformation tensors between the tangent space and the cotangent space in the material configuration, the intermediate configuration and the spatial configuration.

According to the above considerations we introduce the metric tensor  $\hat{\mathbf{G}}$  and the elastic Cauchy-Green tensor

$$\hat{\mathbf{C}} = \mathbf{F}_e^t \cdot \mathbf{g} \cdot \mathbf{F}_e \quad (7)$$

in the intermediate configuration. The correlations between the metric tensors and the deformation tensors are visualised in Fig. 2. The pullback of the spatial velocity gradient in Eq. 5 to the intermediate configuration

$$\hat{\mathbf{L}} = \mathbf{F}_e^{-1} \cdot \mathbf{l} \cdot \mathbf{F}_e = \hat{\mathbf{L}}_e + \hat{\mathbf{L}}_g \quad (8)$$

can additively be split into the elastic velocity gradient and the growth velocity gradient

$$\hat{\mathbf{L}}_e := \mathbf{F}_e^{-1} \cdot \dot{\mathbf{F}}_e \quad \text{and} \quad \hat{\mathbf{L}}_g := \dot{\mathbf{F}}_g \cdot \mathbf{F}_g^{-1}, \quad (9)$$

respectively.

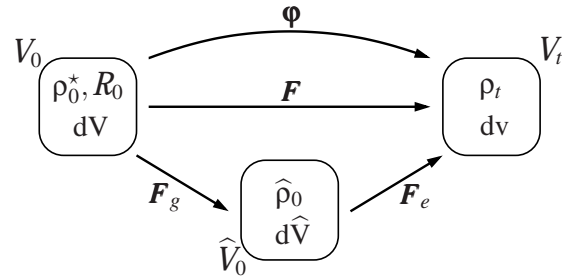


**Figure 3** : The grown mass element  $dm$  consists of the initial mass element  $dM$  and the mass produced by the mass source  $R_0$  during the time interval  $[t, t_0]$ . In the intermediate configuration and in the spatial configuration it can be expressed as the product of the density and the volume element.

## 2.2 Density transformations

In the following section we consider the transformations between the density expressions in different configurations. Herein the scalar value  $\rho_0^*$  signifies the initial density of a mass element. Its counterpart in the spatial configuration and in the intermediate configuration is denoted by  $\rho_t$  and  $\hat{\rho}_0$ , respectively. A volume element in the material configuration is characterised by  $dV$ , its counterpart in the spatial configuration is  $dv$ . In the intermediate configuration the volume element is termed  $d\hat{V}$ . In analogy to the Jacobian  $J = \det \mathbf{F}$  of the total deformation gradient we define the Jacobians  $J_e = \det \mathbf{F}_e > 0$  and  $J_g = \det \mathbf{F}_g > 0$  of the elastic deformation gradient and the growth deformation gradient, respectively. Note that the Jacobian of  $\mathbf{F}$  is the product of the Jacobians of  $\mathbf{F}_e$  and  $\mathbf{F}_g$ , that is  $J = J_e J_g$ . As depicted in Fig. 3 the Jacobians transform the volume element in the well-known form

$$dv = J dV, \quad d\hat{V} = J_g dV, \quad dv = J_e d\hat{V}. \quad (10)$$

With the notations given above we obtain the initial mass element as

$$dM = \rho_0^* dV. \quad (11)$$

In the following  $R_0$  should denote a mass source per unit volume in the material configuration. A mass flux through the surface of the considered mass element will be neglected. Therewith the grown mass element  $dm$  consist of the initial mass element  $dM$  and an additional mass term taking into account the production of mass by

the mass source  $R_0$  during the time interval  $[t_0, t]$

$$dm = dM + \int_{t_0}^t R_0 d\bar{t} dV. \quad (12)$$

In the intermediate configuration, the mass element can also be written as

$$dm = \hat{\rho}_0 d\hat{V}. \quad (13)$$

Since the deformation map between the intermediate configuration and the spatial configuration is a purely elastic map, the mass element expressed in terms of the spatial quantities is

$$dm = \rho_t dv. \quad (14)$$

Insertion of the volume mappings in Eq. 10 into the expressions of the grown mass element in Eq. 13 and Eq. 14 yields the transformation of the density from the spatial to the intermediate state

$$\hat{\rho}_0 = J_e \rho_t. \quad (15)$$

Furthermore, we define the density of the grown mass element in the material configuration

$$\rho_0 := J \rho_t = J_g \hat{\rho}_0. \quad (16)$$

Insertion of Eq. 10, Eq. 11, Eq. 14 and Eq. 16 into Eq. 12 yields the expression

$$\rho_0 = \rho_0^* + \int_{t_0}^t R_0 d\bar{t}, \quad (17)$$

which underlines, that the density of the grown mass element consists of the initial density and a production term taking into account the mass source.

### 2.3 Essential balance equations

The time derivative of Eq. 17 also yields the well known local balance of mass in the material configuration

$$\dot{\rho}_0 = R_0. \quad (18)$$

Insertion of the density transformation in Eq. 16<sub>2</sub> and the definition of the growth velocity gradient in Eq. 9<sub>2</sub> into the local balance of mass in the material configuration Eq. 18 yields the local balance of mass in the intermediate configuration

$$\dot{\hat{\rho}}_0 + \hat{\rho}_0 \text{tr} \hat{\mathbf{L}}_g = J_g^{-1} R_0, \quad (19)$$

with  $J_g = \partial_{\mathbf{F}_g} J_g : \dot{\mathbf{F}}_g = J_g \mathbf{F}_g^{-1} : \dot{\mathbf{F}}_g = J_g \text{tr} \hat{\mathbf{L}}_g$ . Further on we need the local balance of linear momentum

$$\rho_0 \dot{\mathbf{v}} = \rho_0 \mathbf{b}_0 + \text{DIV}(\mathbf{F} \cdot \mathbf{S}), \quad (20)$$

and the entropy inequality

$$\rho_0 D := \frac{1}{2} \mathbf{S} : \dot{\mathbf{C}} - \rho_0 \dot{\psi} - \theta \rho_0 \mathcal{S}_0 \geq 0, \quad (21)$$

where  $\mathbf{b}_0$  denotes the body forces,  $\mathbf{S}$  is the Piola-Kirchhoff stress tensor in the material configuration and  $\psi$  is the free energy per unit mass. The extra entropy term  $\mathcal{S}_0$  is necessary to satisfy the second law of thermodynamics. The balance equations are also discussed in more detail for instance in Epstein & Maugin (2000), Kuhl & Steinmann (2003) and Himpel (2003).

### 2.4 Different cases for mass change

One can distinguish between three cases inducing a mass change. First the density is kept constant, so for a mass change, the volume must change. Second the volume is kept constant, such that the density must change. Third, the density and the volume can change. In the past volume preserving growth models have been applied successfully to simulate porous biomaterials such as hard tissues, see e.g. van Rietbergen et al. (2003). However, for soft tissues, these models seem less appropriate since the addition of new material has an direct impact on the volume of the tissue, see for instance Humphrey (2002).

#### 2.4.1 Density preservation

Assumption of density preservation from the initial state to the intermediate configuration, viz  $\hat{\rho}_0 = \rho_0^* = \text{const}$ , implicates that the volume of the mass element has to change in order to obtain mass change. This effect of a volume change will be denoted as growth if the volume increases or as atrophy if the volume decreases, see also Taber (1995). Insertion of the ansatz of density preservation into the local balance of mass Eq. 19 yields the mass source

$$R_0 = \rho_0 \text{tr} \hat{\mathbf{L}}_g = J_g \rho_0^* \text{tr} \hat{\mathbf{L}}_g. \quad (22)$$

Thus if the growth deformation gradient  $\mathbf{F}_g$  and its evolution  $\dot{\mathbf{F}}_g$  is known, the mass source can be determined directly.

### 2.4.2 Volume preservation

For volume preserving growth, namely  $d\hat{V} = dV = \text{const}$ , the density of the mass element has to change to induce a mass change. This effect will be called remodelling. The determinant of the growth deformation gradient must be  $J_g = 1$  for such an ansatz.

### 2.4.3 Volume and density change

The third case of mass change is the situation where both, the volume and the density are allowed to vary. In that case growth or respectively atrophy and remodelling occur. For a complete description of this model an additional assumption has to be made to describe the form of mass change.

## 3 Constitutive equations

To take into account the characteristic response of a particular material, constitutive equations must be specified. In what follows, we shall restrict ourselves to the modelling of an isotropic response for the sake of clarity. However, an extension to anisotropic elastic behaviour, as documented e.g. by Holzapfel et al. (2000), Holzapfel & Ogden (2003), Kuhl et al. (2004a; 2004) or Menzel (2005; 2005a), does not pose any additional conceptual difficulties. For the discussed case of multiplicative growth the free energy function and an equation describing the form of growth, for example the growth deformation tensor  $\mathbf{F}_g$ , must be provided. Finally, the given constitutive equations will be applied to the cases of a density preserving mass change and a volume preserving mass change.

### 3.1 Free energy

We assume an isotropic free energy density per unit mass  $\psi$  depending on the elastic Cauchy-Green tensor  $\hat{\mathbf{C}}$  and the grown material density  $\rho_0$

$$\psi = \psi(\hat{\mathbf{C}}, \rho_0). \quad (23)$$

From Fig. 2 we can identify  $\hat{\mathbf{C}} = \mathbf{F}_g^{-t} \cdot \mathbf{C} \cdot \mathbf{F}_g^{-1}$ . Insertion of the time derivative of the free energy density

$$\begin{aligned} \dot{\psi} &= \left[ \mathbf{F}_g^{-1} \cdot \frac{\partial \psi}{\partial \hat{\mathbf{C}}} \cdot \mathbf{F}_g^{-t} \right] : \dot{\mathbf{C}} \\ &\quad - \left[ 2\hat{\mathbf{C}} \cdot \frac{\partial \psi}{\partial \hat{\mathbf{C}}} \cdot \mathbf{F}_g^{-t} \right] : \dot{\mathbf{F}}_g + \frac{\partial \psi}{\partial \rho_0} \dot{\rho}_0 \end{aligned} \quad (24)$$

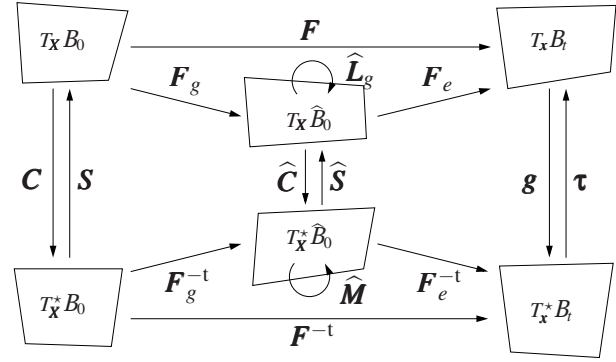


**Figure 4** : Visualisation of the stress tensors and the work conjugated deformation tensors.  $\mathbf{S}$  and  $\hat{\mathbf{S}}$  denote the Piola-Kirchhoff stresses in the material and in the intermediate configuration.  $\boldsymbol{\tau}$  characterises the Kirchhoff stress tensor.

into the entropy inequality Eq. 21 yields the definition of the Piola-Kirchhoff stresses in the material configuration

$$\mathbf{S} := 2\rho_0 \mathbf{F}_g^{-1} \cdot \frac{\partial \psi}{\partial \hat{\mathbf{C}}} \cdot \mathbf{F}_g^{-t} = 2\rho_0 \frac{\partial \psi}{\partial \mathbf{C}} \quad (25)$$

by the standard argumentation of rational mechanics. Accordingly the push forward of the Piola-Kirchhoff stresses to the intermediate configuration follows as

$$\hat{\mathbf{S}} = \mathbf{F}_g \cdot \mathbf{S} \cdot \mathbf{F}_g^t = 2\rho_0 \frac{\partial \psi}{\partial \hat{\mathbf{C}}}. \quad (26)$$

Thus from Eq. 21 we obtain the reduced dissipation inequality

$$\rho_0 D^{red} := \hat{\mathbf{M}} : \hat{\mathbf{L}}_g - \rho_0 \frac{\partial \psi}{\partial \rho_0} R_0 - \theta \rho_0 S_0 \geq 0 \quad (27)$$

with the Mandel stresses  $\hat{\mathbf{M}} = \hat{\mathbf{C}} \cdot \hat{\mathbf{S}}$ , which are work conjugate to the growth velocity gradient  $\hat{\mathbf{L}}_g$  in the intermediate configuration. In Fig. 4 the introduced stresses and their work conjugated quantities are visualised, whereby  $\boldsymbol{\tau} = 2\rho_0 \partial \psi / \partial \mathbf{g} = \mathbf{F} \cdot \mathbf{S} \cdot \mathbf{F}^t$  denotes the Kirchhoff stress tensor.

### 3.2 Growth deformation gradient

Following Lubarda & Hoger (2002), we define the isotropic growth deformation gradient as a multiple of the identity

$$\mathbf{F}_g := \vartheta \mathbf{I} \quad (28)$$

with  $\vartheta$  being the isotropic stretch ratio due to volumetric mass growth. Consequently, the related Jacobian is  $J_g = \vartheta^3$ . Thus the grown density in the material configuration, see Eq. 16, can be expressed as

$$\rho_0 = \vartheta^3 \widehat{\rho}_0. \quad (29)$$

Furthermore the growth velocity gradient in Eq. 9 can be rewritten as

$$\widehat{\mathbf{L}}_g = \frac{\dot{\vartheta}}{\vartheta} \mathbf{I}. \quad (30)$$

### 3.3 Application to different cases for mass change

As mentioned above an additional requirement is needed to describe the form of mass change. In this section the given constitutive equations for the free energy and the growth deformation tensor will be derived for the special cases of the density preserving approach and the volume preserving approach.

#### 3.3.1 Density preservation

For the density preserving case, i.e.  $\widehat{\rho}_0 = \rho_0^* = \text{const}$ , Eq. 29 can be rewritten as

$$\rho_0 = \vartheta^3 \rho_0^*. \quad (31)$$

From the local balance of mass, see Eq. 18, or alternatively from Eq. 22 the mass source follows straightforwardly as

$$\mathbf{R}_0 = \mathbf{j}_g \rho_0^* = 3\rho_0^* \vartheta^2 \dot{\vartheta}. \quad (32)$$

Thus for density preservation the mass source  $\mathbf{R}_0$  and therewith the evolution of the density is clearly driven by the evolution of the stretch ratio

$$\dot{\vartheta} = f_\vartheta(\vartheta, \text{tr} \widehat{\mathbf{M}}), \quad (33)$$

which are assumed to depend on the stretch ratio itself and the trace of the Mandel stresses  $\widehat{\mathbf{M}}$ . In contrast to Lubarda & Hoger (2002), who chose a dependence on the Piola-Kirchhoff stresses, we prefer the ansatz in Eq. 33, since the Mandel stresses  $\widehat{\mathbf{M}}$  are energetically conjugated to the growth velocity gradient  $\widehat{\mathbf{L}}_g$ , see Eq. 27. Conceptually speaking,  $\text{tr} \widehat{\mathbf{M}}$  equals  $\text{tr} \boldsymbol{\tau}$  which takes the interpretation as a representative scalar of the volumetric stress contribution. The simplest form of Eq. 33 is a linear dependence of  $\dot{\vartheta}$  on the trace of the Mandel stresses

$$\dot{\vartheta} = k_\vartheta(\vartheta) \text{tr} \widehat{\mathbf{M}}. \quad (34)$$

Following Lubarda & Hoger (2002), the coefficient  $k_\vartheta$  is introduced as

$$\begin{aligned} k_\vartheta(\vartheta) &= k_\vartheta^+ \left[ \frac{\vartheta^+ - \vartheta}{\vartheta^+ - 1} \right]^{m_\vartheta^+} && \text{for } \text{tr} \widehat{\mathbf{M}} > 0 \\ k_\vartheta(\vartheta) &= k_\vartheta^- \left[ \frac{\vartheta - \vartheta^-}{1 - \vartheta^-} \right]^{m_\vartheta^-} && \text{for } \text{tr} \widehat{\mathbf{M}} < 0 \end{aligned} \quad (35)$$

to prevent unlimited growth. Herein the parameters  $\vartheta^+ > 1$  and  $\vartheta^- < 1$  denote the limiting values of the stretch ratios that can be reached by growth and atrophy, respectively. The parameters  $k_\vartheta^+$ ,  $m_\vartheta^+$  and  $k_\vartheta^-$ ,  $m_\vartheta^-$  are constant material parameters.

Moreover the free energy density per unit volume  $\psi_0$  is assumed to depend on the elastic Cauchy-Green tensor  $\widehat{\mathbf{C}}$  or respectively on the invariants  $I_{i=1,2,3}$  of  $\widehat{\mathbf{C}}$

$$\psi = \psi(\widehat{\mathbf{C}}, \rho_0) = \frac{1}{\rho_0} \psi_0(\widehat{\mathbf{C}}) = \frac{1}{\rho_0} \psi_0(I_1, I_2, I_3), \quad (36)$$

so that isotropic response is captured. Therewith the Piola-Kirchhoff stresses in the material configuration and in the intermediate configuration become

$$\mathbf{S} = 2 \frac{\partial \psi_0}{\partial \widehat{\mathbf{C}}} \quad \text{and} \quad \widehat{\mathbf{S}} = 2 \frac{\partial \psi_0}{\partial \widehat{\mathbf{C}}}. \quad (37)$$

Furthermore with Eq. 28, Eq. 31, Eq. 32 and Eq. 30 the reduced dissipation inequality in Eq. 27 can be reformulated as

$$\rho_0 D^{red} := \frac{k_\vartheta(\vartheta)}{\vartheta} \text{tr} \widehat{\mathbf{M}} \left[ \text{tr} \widehat{\mathbf{M}} + 3\psi_0 \right] - \theta \vartheta^3 \rho_0^* \mathcal{S}_0 \geq 0. \quad (38)$$

Therefrom the extra entropy source follows as

$$\mathcal{S}_0 \leq \frac{k_\vartheta(\vartheta) \text{tr} \widehat{\mathbf{M}}}{\theta \rho_0^* \vartheta^4} \left[ \text{tr} \widehat{\mathbf{M}} + 3\psi_0 \right]. \quad (39)$$

#### 3.3.2 Volume preservation

As aforementioned for the volume preserving case, i.e.  $d\widehat{\mathbf{V}} = d\mathbf{V} = \text{const}$ , the Jacobian of the growth deformation tensor must be  $J_g = 1$ . Thus, with the definition in Eq. 28, the isotropic stretch ratio must be  $\vartheta = 1$ . This leads to the deformation gradients

$$\mathbf{F}_g = \mathbf{I} \quad \text{and} \quad \mathbf{F}_e = \mathbf{F}. \quad (40)$$

The assumed growth deformation tensor in Eq. 28 under volume preservation renders the material configuration to

coincide with the intermediate configuration. The intermediate configuration is thus dispensable. Since in this particular case changes in mass follow exclusively from changes in density, a mass source can be specified constitutively. Following Harrigan & Hamilton (1992; 1993), the mass source is defined as

$$\mathbf{R}_0 = \left[ \frac{\rho_0}{\rho_0^*} \right]^{-m} \psi_0 - \psi_0^*, \quad (41)$$

with the stress stimulus attractor  $\psi_0^*$  indicating the point where the density rate becomes zero, see Beaupré et al. (1990). Moreover the free energy density is based on an elastic free energy weighted by the relative density  $[\rho_0/\rho_0^*]^n$

$$\begin{aligned} \psi &= \psi(\mathbf{C}, \rho_0) = \left[ \frac{\rho_0}{\rho_0^*} \right]^n \psi^E(\widehat{\mathbf{C}}, \rho_0) \\ &= \left[ \frac{\rho_0}{\rho_0^*} \right]^n \frac{1}{\rho_0} \psi_0^E(\widehat{\mathbf{C}}). \end{aligned} \quad (42)$$

Again a formulation depending on the invariants is possible. Therewith the Piola-Kirchhoff stresses become

$$\mathbf{S} = \left[ \frac{\rho_0}{\rho_0^*} \right]^n 2 \frac{\partial \psi_0^E}{\partial \mathbf{C}} = \left[ \frac{\rho_0}{\rho_0^*} \right]^n \mathbf{S}^E. \quad (43)$$

For the reduced dissipation inequality in Eq. 27 we obtain

$$\rho_0 D^{red} := [1 - n] \psi \left[ \left[ \frac{\rho_0}{\rho_0^*} \right]^{-m} \psi_0 - \psi_0^* \right] - \theta \rho_0 \mathcal{S}_0 \geq 0 \quad (44)$$

so that the extra entropy source follows as

$$\mathcal{S}_0 \leq \frac{1}{\theta} [1 - n] \psi \left[ \left[ \frac{\rho_0}{\rho_0^*} \right]^{-m} \psi_0 - \frac{1}{\rho_0} \psi_0^* \right]. \quad (45)$$

The theory and implementation for such a material model is discussed in more detail for instance in Kuhl et al. (2003) and Himpel (2003).

#### 4 Numerical implementation

In this section we concentrate on the numerical implementation of the discussed constitutive theory for the density preserving case. The implementation of the volume preserving case has been discussed in the above given literature. As we assume no mass flux but solely a mass source, we can apply standard finite element techniques based on an internal variable formulation for the stretch ratio.

##### 4.1 Incremental tangent modulus

For the computation of the discussed material model we first develop the tangent modulus at the spatial time step. Since the material model is formulated with respect to the intermediate configuration, the corresponding tangent modulus is defined in terms of stresses and strains in the intermediate configuration, for instance the Piola-Kirchhoff stresses  $\widehat{\mathbf{S}}$  in Eq. 26 and the elastic Cauchy-Green tensor  $\widehat{\mathbf{C}}$  in Eq. 7. By application of the chain rule we obtain the incremental elastic-growth tangent modulus in the intermediate configuration at the spatial time step

$$\widehat{\mathbb{C}}_{n+1}^{eg} = 2 \frac{d\widehat{\mathbf{S}}_{n+1}}{d\widehat{\mathbf{C}}_{n+1}} = 2 \frac{\partial \widehat{\mathbf{S}}_{n+1}}{\partial \widehat{\mathbf{C}}_{n+1}} + 2 \frac{\partial \widehat{\mathbf{S}}_{n+1}}{\partial \vartheta_{n+1}} \otimes \frac{\partial \vartheta_{n+1}}{\partial \widehat{\mathbf{C}}_{n+1}}. \quad (46)$$

For the sake of clarity we will drop the index  $n+1$  for the time step in the following. In Eq. 46 the partial derivative of the stresses with respect to the strains denotes the elastic tangent modulus in the intermediate configuration

$$\widehat{\mathbb{C}}^e := 4 \frac{\partial^2 \psi_0}{\partial \widehat{\mathbf{C}}^2} = 2 \frac{\partial \widehat{\mathbf{S}}}{\partial \widehat{\mathbf{C}}}. \quad (47)$$

In order to determine the second part of Eq. 46<sub>2</sub>, we again apply the chain rule

$$2 \frac{\partial \widehat{\mathbf{S}}}{\partial \vartheta} = 2 \frac{\partial \widehat{\mathbf{S}}}{\partial \widehat{\mathbf{C}}} : \frac{\partial \widehat{\mathbf{C}}}{\partial \vartheta} = -\frac{2}{\vartheta} \widehat{\mathbb{C}}^e : \widehat{\mathbf{C}}, \quad (48)$$

whereby  $\partial \widehat{\mathbf{C}} / \partial \vartheta = \partial(\mathbf{F}_g^{-t} \cdot \mathbf{C} \cdot \mathbf{F}_g^{-1}) / \partial \vartheta = -2\vartheta^{-3} \mathbf{C} = -2\vartheta^{-1} \widehat{\mathbf{C}}$ . The computation of the third part of Eq. 46<sub>2</sub> is not straightforward since solely the evolution of the stretch ratio is known, but not the stretch ratio itself. Therefore we apply an implicit Euler backward scheme to obtain the stretch ratio at the spatial time step

$$\vartheta = \vartheta_n + \dot{\vartheta} \Delta t, \quad (49)$$

and differentiate this equation with respect to the elastic Cauchy-Green tensor

$$\frac{\partial \vartheta}{\partial \widehat{\mathbf{C}}} = \left[ \frac{\partial \dot{\vartheta}}{\partial \widehat{\mathbf{C}}} + \frac{\partial \dot{\vartheta}}{\partial \vartheta} \frac{\partial \vartheta}{\partial \widehat{\mathbf{C}}} \right] \Delta t. \quad (50)$$

Solving this equation for the derivative of the stretch ratio with respect to the elastic Cauchy-Green strains yields

$$\frac{\partial \vartheta}{\partial \widehat{\mathbf{C}}} = \frac{1}{\partial \vartheta \dot{\vartheta}}^{-1} \frac{\partial \dot{\vartheta}}{\partial \widehat{\mathbf{C}}} \Delta t \quad (51)$$

with the abbreviation

$$\begin{aligned} \overline{\partial_\vartheta \dot{\vartheta}} &:= 1 - \frac{\partial \dot{\vartheta}}{\partial \vartheta} \Delta t \\ &= 1 - \left[ \frac{\partial k_\vartheta}{\partial \vartheta} \widehat{\mathbf{M}} + k_\vartheta(\vartheta) \frac{\partial \widehat{\mathbf{M}}}{\partial \vartheta} \right] \Delta t. \end{aligned} \quad (52)$$

Recall from Eq. 35 that we have to distinguish between tensile and compressive stress states for the partial derivative of the coefficient  $k_\vartheta$  with respect to the stretch ratio

$$\begin{aligned} \frac{\partial k_\vartheta}{\partial \vartheta} &= \frac{m_\vartheta^+}{\vartheta - \vartheta^+} k_\vartheta(\vartheta) \quad \text{for } \widehat{\mathbf{M}} > 0, \\ \frac{\partial k_\vartheta}{\partial \vartheta} &= \frac{m_\vartheta^-}{\vartheta - \vartheta^-} k_\vartheta(\vartheta) \quad \text{for } \widehat{\mathbf{M}} < 0. \end{aligned} \quad (53)$$

The partial derivative of  $\widehat{\mathbf{M}}$  with respect to  $\vartheta$  results in

$$\frac{\partial \widehat{\mathbf{M}}}{\partial \vartheta} = -\frac{1}{\vartheta} \left[ 2 \widehat{\mathbf{M}} + \widehat{\mathbf{C}} : \widehat{\mathbf{C}}^e : \widehat{\mathbf{C}} \right] \quad (54)$$

with the elastic tangent modulus being defined in Eq. 47. Finally, the second term in Eq. 51 can directly be determined as

$$\frac{\partial \dot{\vartheta}}{\partial \widehat{\mathbf{C}}} = k_\vartheta(\vartheta) \frac{\partial \widehat{\mathbf{M}}}{\partial \widehat{\mathbf{C}}} = k_\vartheta(\vartheta) \left[ \widehat{\mathbf{S}} + \frac{1}{2} \widehat{\mathbf{C}} : \widehat{\mathbf{C}}^e \right]. \quad (55)$$

Summarising the unsymmetric elastic-growth tangent modulus reads

$$\begin{aligned} \widehat{\mathbf{C}}_{n+1}^{eg} &= \widehat{\mathbf{C}}_{n+1}^e - \frac{2}{\vartheta_{n+1}} \overline{\partial_\vartheta \dot{\vartheta}}^{-1} k_\vartheta(\vartheta_{n+1}) \Delta t \\ &\quad \left[ \widehat{\mathbf{C}}_{n+1}^e : \widehat{\mathbf{C}}_{n+1} \right] \otimes \left[ \widehat{\mathbf{S}}_{n+1} + \frac{1}{2} \widehat{\mathbf{C}}_{n+1} : \widehat{\mathbf{C}}_{n+1}^e \right]. \end{aligned} \quad (56)$$

#### 4.2 Incremental update of the stretch ratio

As we can identify from the previous section, the tangent modulus, see Eq. 56, and therewith the stresses depend on the stretch ratio at the spatial time step. From Eq. 31 we conclude that the spatial density  $\rho_t$  depends solely on the stretch ratio for density preservation. Consequently it proves convenient to introduce  $\vartheta$  as internal variable. In order to compute the stretch ratio at the spatial time step we incorporate the implicit Euler backward scheme, see Eq. 49, and formulate the residual

$$R_\vartheta = -\vartheta + \vartheta_n + k_\vartheta(\vartheta) \widehat{\mathbf{M}} \Delta t = 0, \quad (57)$$

which has to vanish in the solution point. Due to the non-linearity of this equation, we will solve it by application of a Newton iteration scheme. Therefore we reformulate Eq. 57 in terms of Taylor series at  $\vartheta$

$$R_\vartheta^{k+1} = R_\vartheta^k - \Delta \vartheta + \frac{\partial \dot{\vartheta}}{\partial \vartheta^k} \Delta \vartheta \Delta t = 0. \quad (58)$$

Solving this equation for the increment  $\Delta \vartheta$  leads to

$$\Delta \vartheta = \overline{\partial_\vartheta \dot{\vartheta}}^{-1} R_\vartheta^k, \quad (59)$$

with the abbreviation  $\overline{\partial_\vartheta \dot{\vartheta}}$  being defined in Eq. 52. There-with we obtain the algorithm

$$\vartheta^{k+1} = \vartheta^k + \Delta \vartheta \quad (60)$$

to update the stretch ratio until a convergence criterion is reached. A summary of the algorithm is given in Tab. 1.

## 5 Numerical examples

In this section the presented theory of multiplicative growth will be discussed for the density preserving case by means of numerical examples. The behaviour of the material model will be elaborated by a simple tension test and a cylindrical tube.

As mentioned above, constitutive equations for the free energy and for the growth deformation gradient must be specified. The growth deformation tensor is clearly indicated by Eq. 28, Eq. 34 and Eq. 35. Furthermore, we choose a free energy function of Neo-Hooke type

$$\psi_0 = \frac{\lambda}{8} \ln^2 I_3 + \frac{\mu}{2} [I_1 - 3 - \ln I_3], \quad (61)$$

with the invariants  $I_1 = \text{tr} \widehat{\mathbf{C}}$  and  $I_3 = \det \widehat{\mathbf{C}}$ .

### 5.1 Simple tension

At first we consider the behaviour of the material model at a stepwise increasing elongation of a one-dimensional bar as depicted in Fig. 5.a. Herein we choose the elastic parameters  $E = 1\text{N/mm}^2$  and  $\nu = 0.3$ , corresponding to  $\lambda = 0.577\text{N/mm}^2$  and  $\mu = 0.385\text{N/mm}^2$ . The initial density is  $\rho_0^* = 1\text{g/cm}^3$ . Unless otherwise stated, the limiting values of the stretch ratio are  $\vartheta^+ = 1.3$  for growth and  $\vartheta^- = 0.5$  for atrophy and the remaining material parameters in Eq. 35 are  $k_\vartheta^+ = 1.0$ ,  $k_\vartheta^- = 2.0$ ,  $m_\vartheta^+ = 2.0$  and

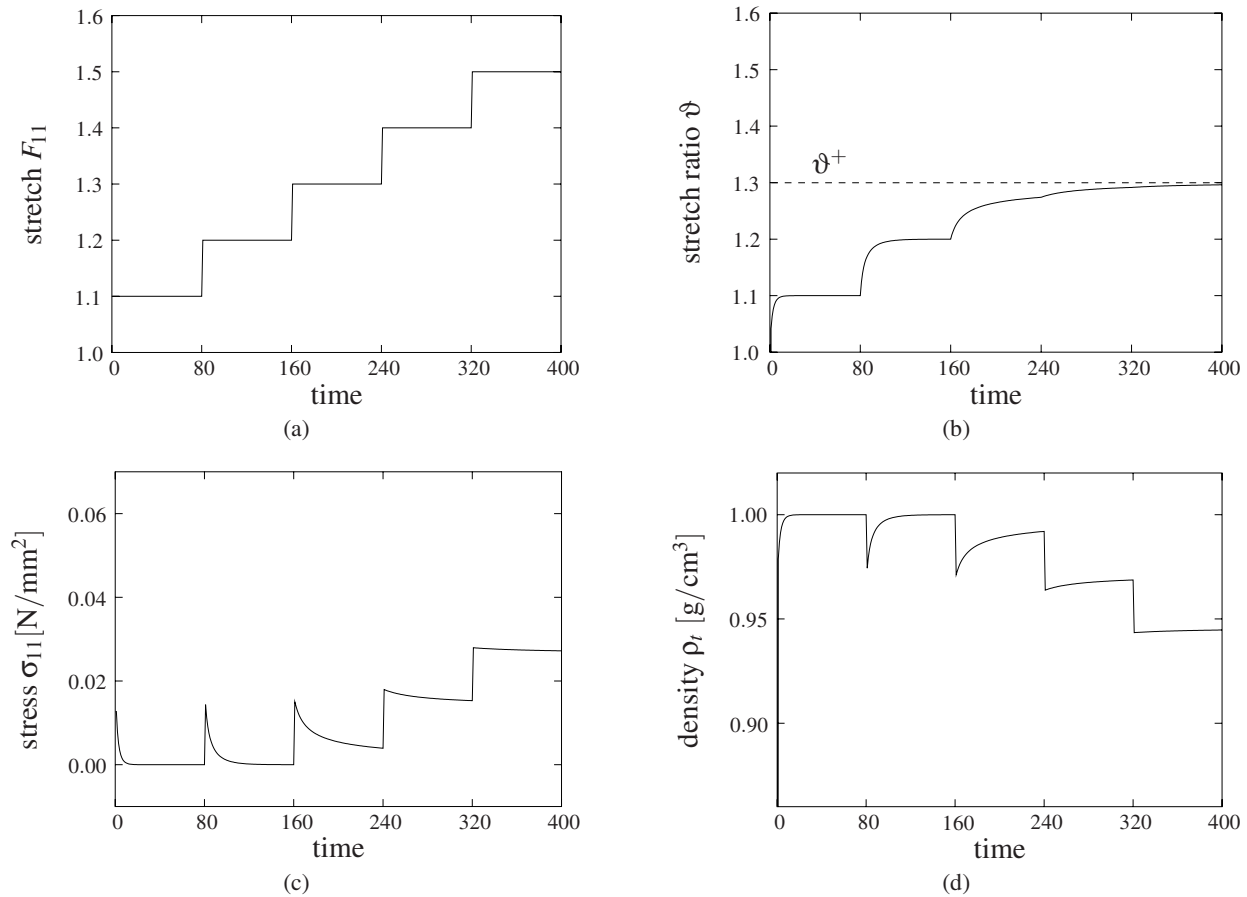


**Figure 5** : a) Application of incrementally increasing stretch. b) Relaxation to a *biological equilibrium*; Limited Growth. c) Stresses vanish in biological equilibrium for  $\vartheta < \vartheta^+$ . d) Density in biological equilibrium does not change for  $\vartheta < \vartheta^+$ .

$m_{\vartheta}^- = 3.0$ . For the time step we choose  $\Delta t = 1.0$ . As one can see in Fig. 5.b the stretch ratio  $\vartheta$  increases at every elongation step until the limiting stretch ratio  $\vartheta^+$  is reached. This means that for  $\vartheta = \vartheta^+$  the evolution of the stretch ratio, see Eq. 34 and Eq. 35, becomes  $\dot{\vartheta} = 0$ . The stretch ratio does not increase instantaneously, although the stretch obviously is applied at once, rather it converges progressively time-depending to the so-called biological equilibrium. The biological equilibrium is defined as the state, where the stretch ratio remains constant and therewith neither the density nor the stresses in the considered specimen changes unless an additional load is applied. Until the limiting stretch ratio is not reached, viz  $\vartheta \neq \vartheta^+$ , we can identify from Eq. 34 and Eq. 35, that the trace of the Mandel stresses must vanish in the biological equilibrium state. This effect can be observed in Fig. 5.c which displays the evolution of the normal

stresses in stretch direction. The normal stresses in the other directions are zero due to the boundary conditions. With Eq. 31 and Eq. 16 the spatial density

$$\rho_t = J^{-1} \vartheta^3 \rho_0^* \quad (62)$$

can be computed. Its evolution is depicted in Fig. 5.d. Obviously the density in the biological equilibrium does not change until the limiting value of the stretch ratio is reached.

Fig. 6 underlines the fact, that  $\vartheta^+$  limits the effect of growth. Until the stretch ratio is lower than the limiting value in the biological equilibrium the applied stretches will be completely compensated by growth. This means that the stretch ratio and therewith the volume of the specimen changes. The density in the biological equilibrium state is equal to the initial density and the stresses are zero. Once the limit of growth is reached, purely elas-

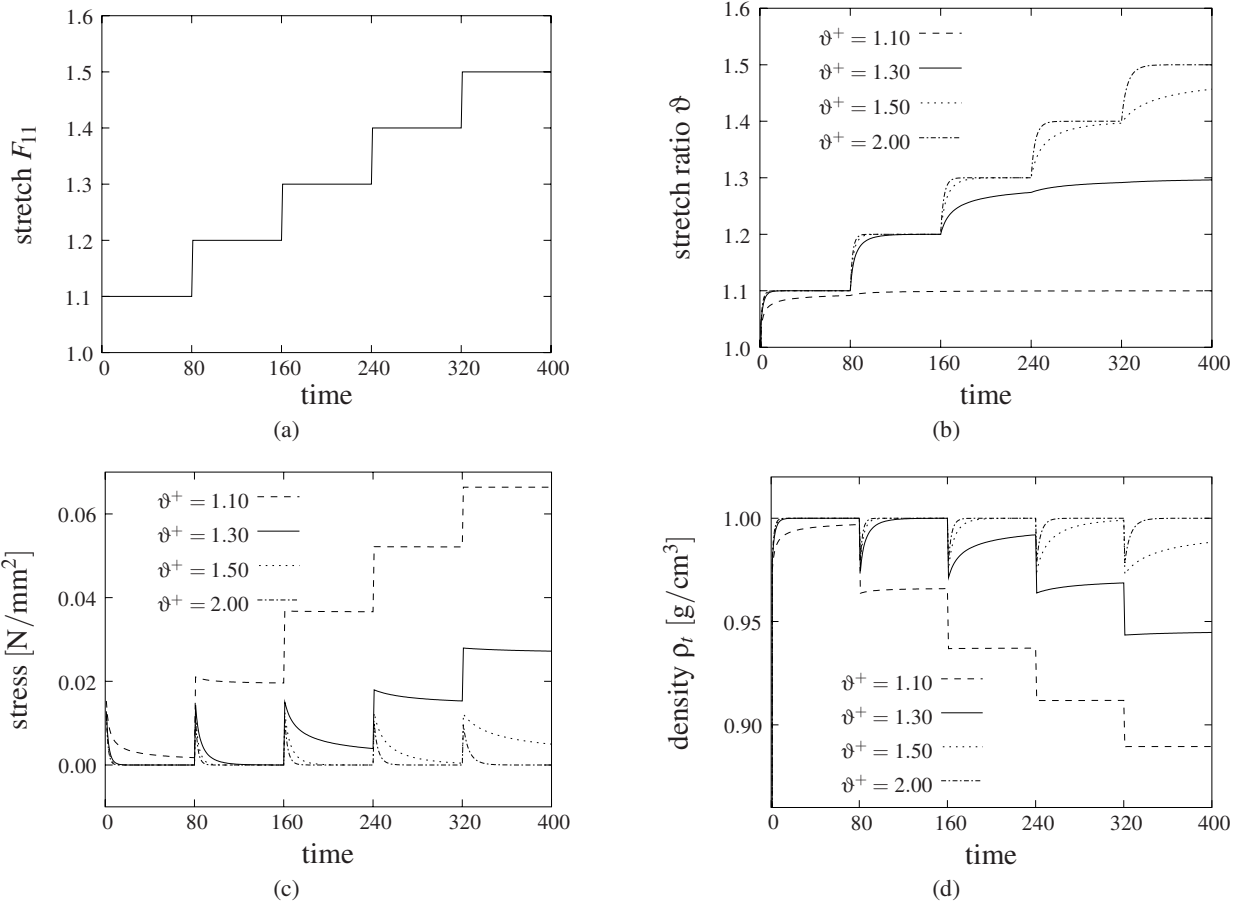


**Figure 6 :** The stretch ratio increases until the limiting value is reached. If the limiting value of the stretch ratio is reached the material behaviour is purely elastic.

tic response can be observed. In Fig. 7 the sensitivity of the material behaviour with respect to the material parameters  $k_{\vartheta}^+$  and  $m_{\vartheta}^+$  is illustrated. Obviously a variation of these parameters influences the relaxation time, but not the final state at biological equilibrium.

For higher values of  $k_{\vartheta}^{\pm}$  the evolution of the stretch ratio in Eq. 34 and Eq. 35 becomes higher. Since  $(\vartheta^+ - \vartheta)/(\vartheta^+ - 1)$  and  $(\vartheta - \vartheta^-)/(1 - \vartheta^-)$  are always smaller than one, the evolution of the stretch ratio becomes higher for smaller values of  $m_{\vartheta}^{\pm}$ . Consequently, the attainment of biological equilibrium is more rapid for high values of  $k_{\vartheta}^{\pm}$  and small values of  $m_{\vartheta}^{\pm}$ . The limiting value  $\vartheta^-$  and the parameters  $k_{\vartheta}^-$  and  $m_{\vartheta}^-$  are not activated for the problem at hand, since solely monotonic loading under tension is considered. It can be shown that for the application of compression a variation of the appropriate parameters will have an analogous effect.

For a better illustration of the fact, that the material

behaviour is purely elastic once the limiting value is reached, we apply a stepwise alternating stretch and compression in a second simulation as illustrated in Fig. 8. Herein we choose the same material parameters as for the first simulation, but limiting values of the stretch ratio of  $\vartheta^+ = 1.1$  for growth and  $\vartheta^- = 0.5$  for atrophy and material parameters  $k_{\vartheta}^+ = 2.0$ ,  $k_{\vartheta}^- = 0.5$ ,  $m_{\vartheta}^+ = 1.0$  and  $m_{\vartheta}^- = 4.0$ .

In the first loading step we apply a stretch of 10%, so that the limiting stretch ratio is reached. This means that the stresses become zero in the biological equilibrium state and the stretch is compensated completely by growth. In the second step we apply a compression of 5% of the initial length, thus the stretch ratio decreases until a new biological equilibrium state is reached. Herein the stresses vanish again. Then we stretched the specimen to the 1.1-fold initial length and obtain the same conditions as in the first loading step. Now the extra stretch of this configu-

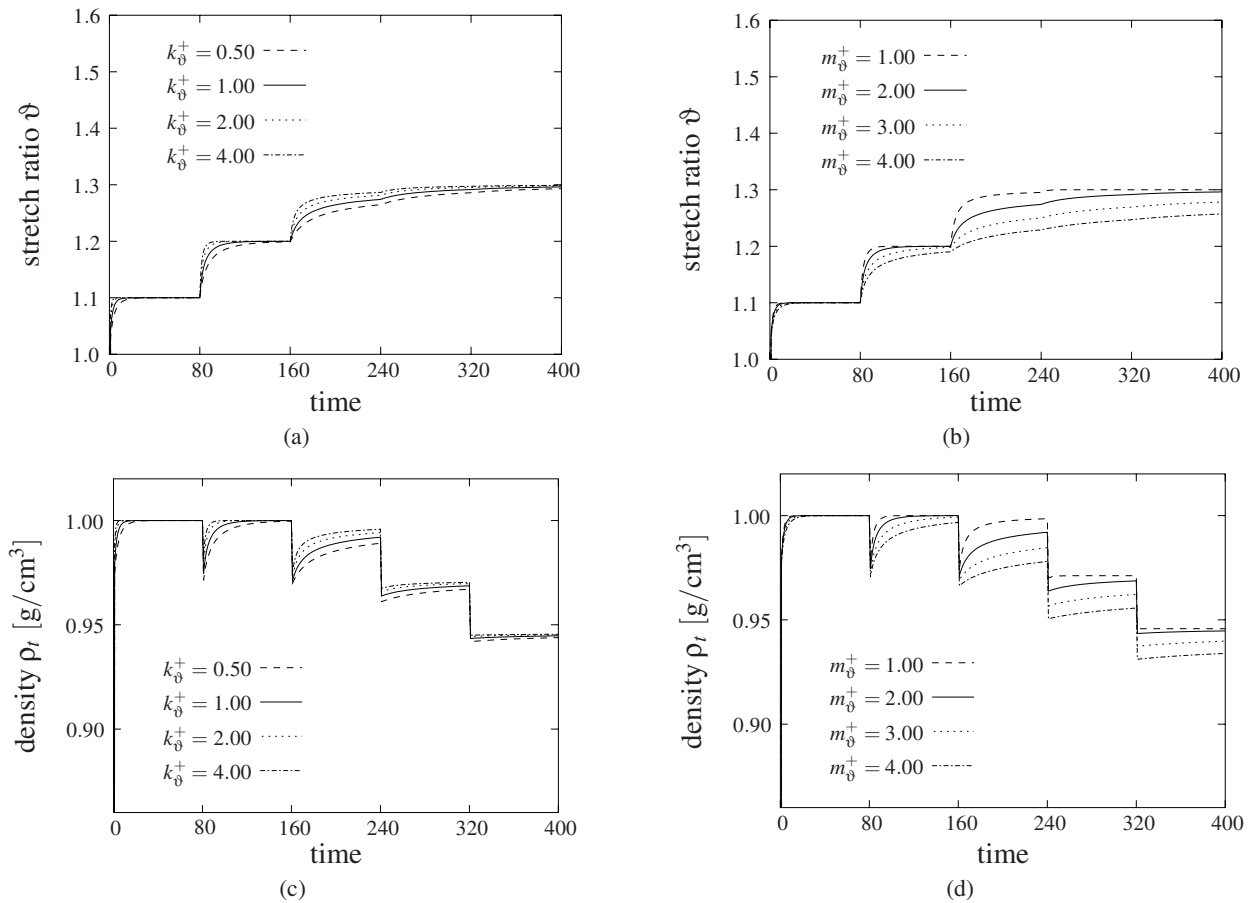


**Figure 7** : The material parameters  $k_{\vartheta}^+$  and  $m_{\vartheta}^+$  influence the relaxation time, but not the final state at biological equilibrium

ration can no longer be compensated by growth, since the limit has already been reached. Thus the stretch in the fourth loading step causes a purely elastic material-behaviour. The stresses are no longer identical to zero. Consequently the displacement in the last loading step of this simulation results in a reduction of elastic strains.

## 5.2 Cylindrical tube

In this section the material model is applied to a cylindrical tube, for instance a stylised blood vessel.

### 5.2.1 Homogeneous loading

In this section a homogeneous deformation of the tube will be considered. Identical constitutive equations as for the simple tension test are applied, i.e. Eq. 28, Eq. 34 and Eq. 35 for the growth deformation tensor and Eq. 61 for the free energy function. The elastic parameters are  $E = 3\text{N/mm}^2$  and  $\nu = 0.3$ , corresponding to

$\lambda = 1.731\text{N/mm}^2$  and  $\mu = 1.154\text{N/mm}^2$ . The initial material density is  $\rho_0^* = 1\text{g/cm}^3$ . The material parameters describing the growth are the limiting values  $\vartheta^+ = 1.5$  and  $\vartheta^- = 0.5$ , the coefficients  $k_{\vartheta}^+ = 0.5$  and  $k_{\vartheta}^- = 0.25$  as well as the exponents  $m_{\vartheta}^+ = 4.0$  and  $m_{\vartheta}^- = 5.0$ . The time iteration has been executed with time steps  $\Delta t = 0.1$ . The discretisation and boundary conditions are depicted in Fig. 9. The lower boundary is fixed in axial and radial direction.

In the first simulation the tube will be stretched in one time step half the initial length in axial direction and then be fixed in this position, which means that the top displacement depicted in Fig. 9 is  $u = 0.5$  during the whole simulation. The initial configuration and the resulting deformations after 1, 100 and 200 time steps as well as the evolution of the stretch ratio are depicted in Fig. 10. At the first loading step the cross section of the tube decreases due to the classical Poisson effect. Then as a re-

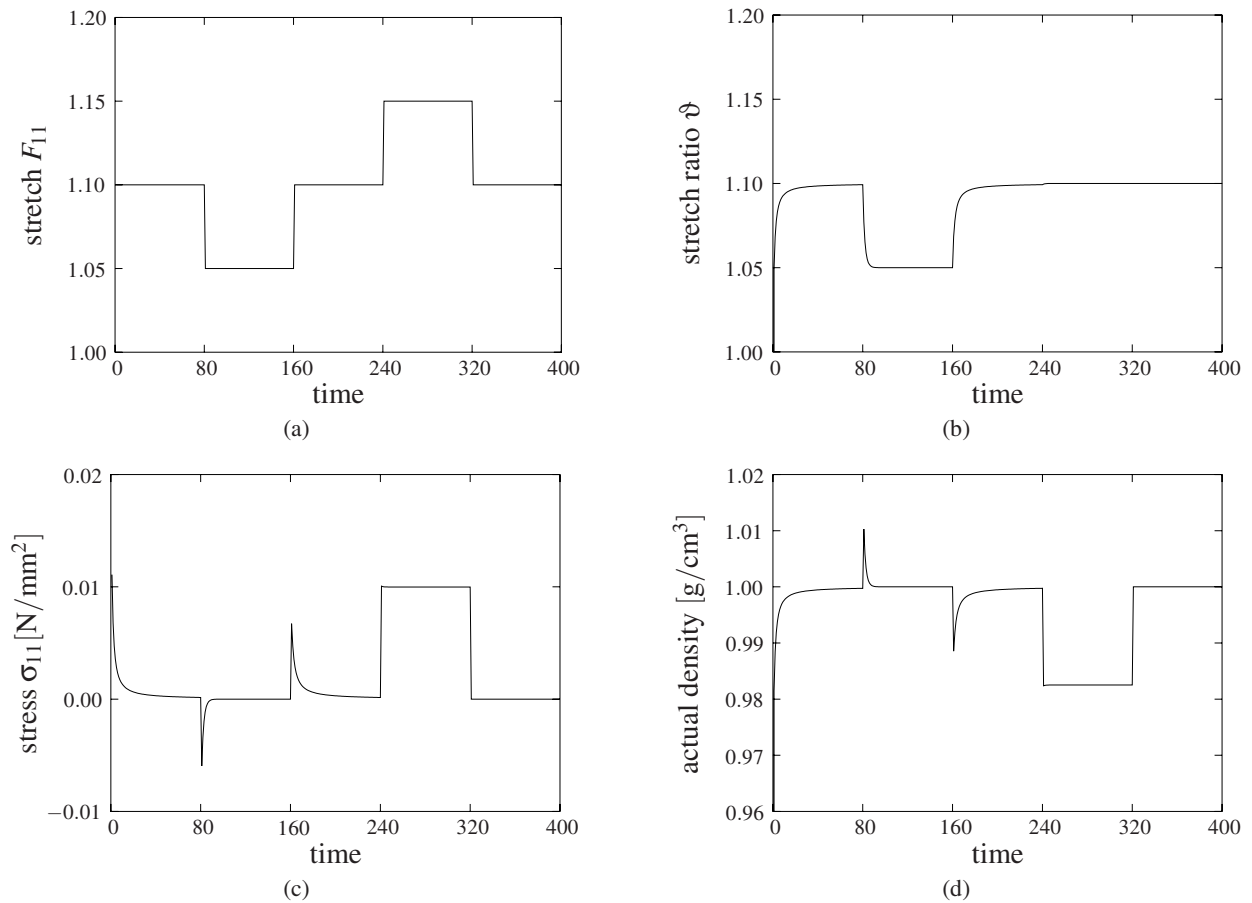


**Figure 8** : Application of stepwise alternating stretch and compression. Until the limiting stretch ratio is not reached, the specimen will grow . Once the limiting value is reached, a purely elastic behaviour can be observed.

result of tension the material grows, this means both the radius and the thickness of the tube become larger. For the first 100 time steps the growth effect is obviously much higher than for the following 100 time steps. This reflects that the density relaxes to a biological equilibrium. This effect can also be seen in Fig. 11.a, where the displacements of the two points  $P_1$  and  $P_2$ , as depicted in Fig. 9, are plotted over time.

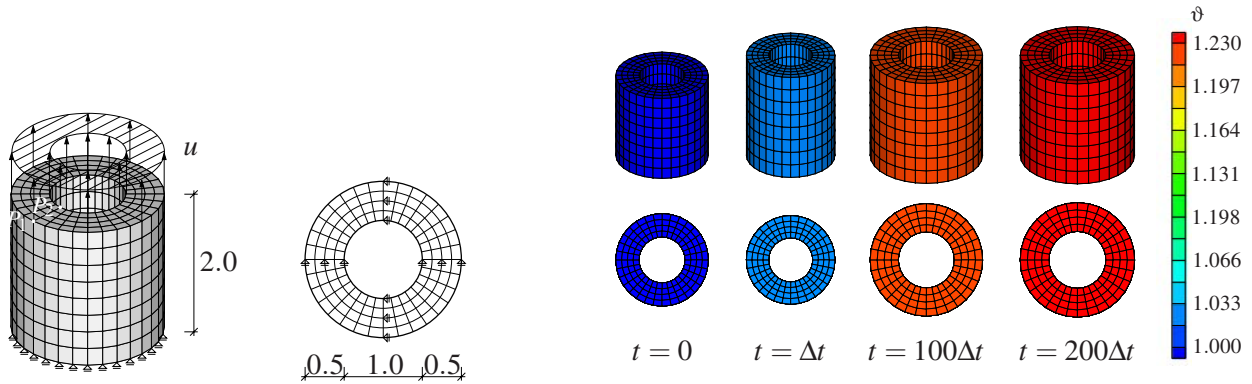
In the second simulation the displacement depicted in Fig. 9 is  $u = -0.5$ . Apparently we apply a constant compression to the tube. In Fig. 12 the initial configuration and the resulting deformations after 1, 100 and 200 time steps are pictured as well as the evolution of the stretch ratio.

Herein we observe the inverse attitude as in Fig. 10. Due to the compression at the first step, reproducing the elasticity of the material, the tube becomes wider. As a result of atrophy both the thickness and the radius become

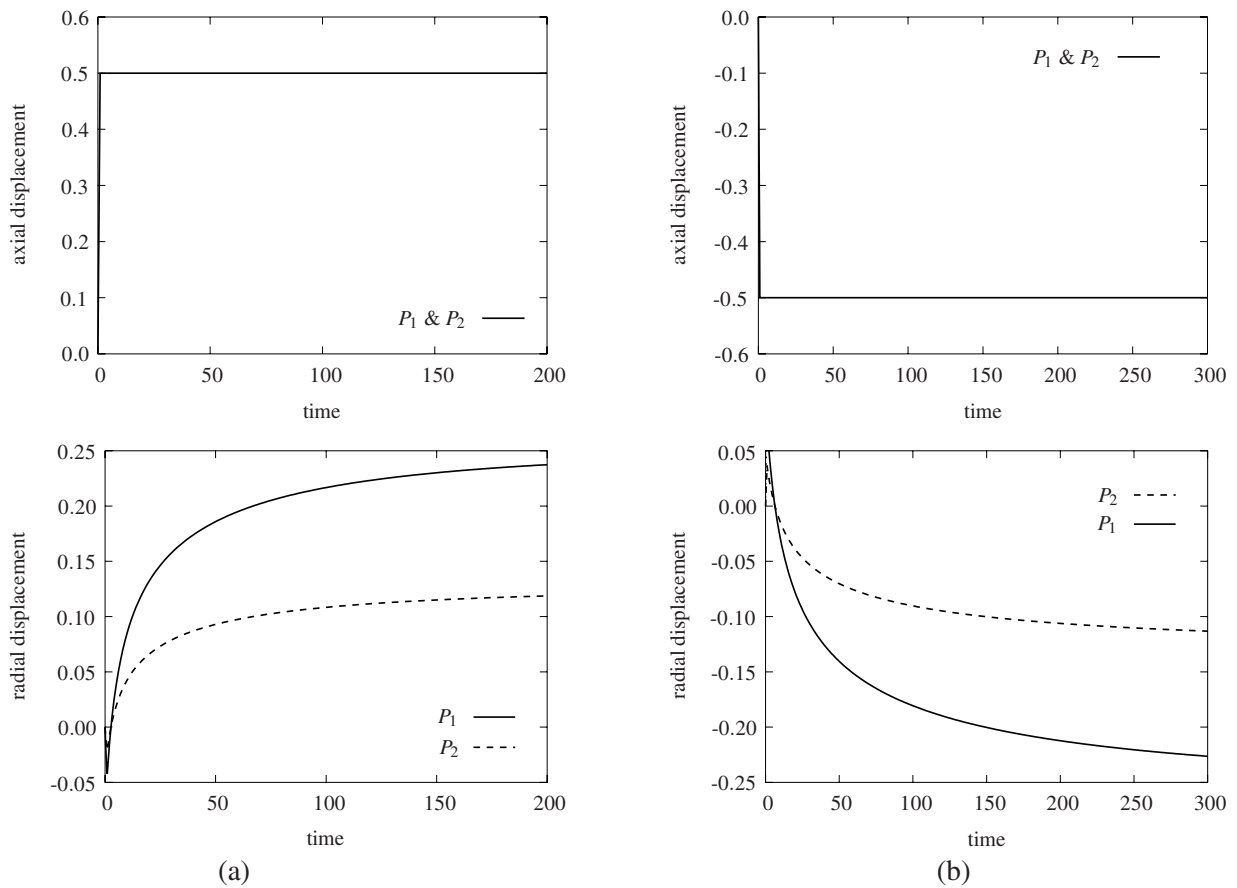
smaller in the long run. Furthermore the relaxing behaviour of the material can again be observed. For this simulation the axial and radial displacement of the two points  $P_1$  and  $P_2$  are plotted against the time in Fig. 11.b. Comparison of the evolution of the radial displacements in Fig. 11 for tension and compression shows the influence of the material parameters  $m_{\vartheta}^{\pm}$  and  $k_{\vartheta}^{\pm}$ . Because of  $m_{\vartheta}^{+} < m_{\vartheta}^{-}$  and  $k_{\vartheta}^{+} > k_{\vartheta}^{-}$ , the relaxation time to the biological equilibrium is smaller in tension than in compression.

### 5.2.2 Inhomogeneous loading

Finally we consider an inhomogeneous deformation of the tube. The discretisation and the boundary conditions are similar to those in the last section, but now both the lower and the upper boundary of the tube are fixed in axial and radial direction. The constitutive equations and material parameters are identical, too. We apply a radial deformation, with peak value at the middle layer of the

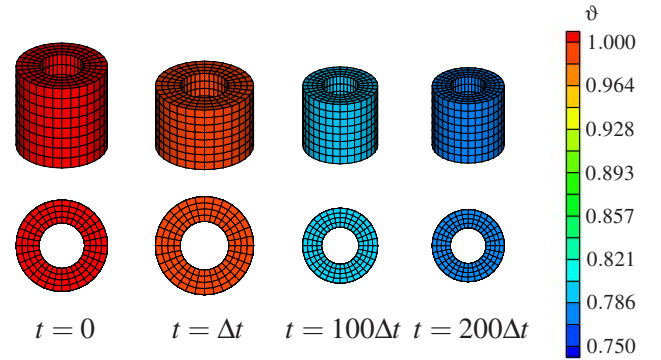
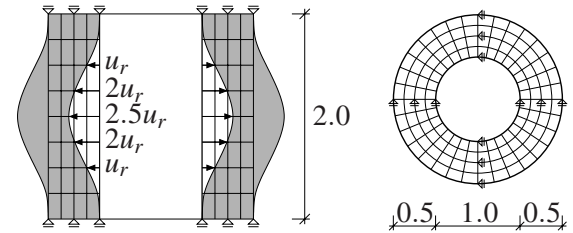


**Figure 9** : Discretisation, load and boundary conditions of the cylindrical tube. **Figure 10** : Deformation of the tube and evolution of the stretch ratio for an axial stretch  $u = 0.5$ .



**Figure 11** : Axial and radial displacements of the points  $P_1$  at the outer boundary of the tube and  $P_2$  at the inner boundary of the tube for (a) tension and (b) compression.

<p>history data: internal variable <math>\vartheta_n</math></p> <ol style="list-style-type: none"> <li>set initial values           <math display="block">\mathbf{F}_e = \mathbf{F} \cdot \mathbf{F}_{gn}^{-1} = \frac{1}{\vartheta_n} \mathbf{F}; \quad \widehat{\mathbf{C}} = \mathbf{F}_e^t \cdot \mathbf{F}_e</math> <math display="block">\widehat{\mathbf{S}} = 2 \frac{\partial \psi_0}{\partial \widehat{\mathbf{C}}}; \quad \widehat{\mathbf{M}} = \widehat{\mathbf{C}} \cdot \widehat{\mathbf{S}}</math> <math display="block">\vartheta = \vartheta_n</math> </li> <li>check loading           <p>IF <math>\text{tr} \widehat{\mathbf{M}} &gt; 0</math> THEN</p> <p>apply <math>k_\vartheta(\vartheta)</math> and <math>\frac{\partial k_\vartheta(\vartheta)}{\partial \vartheta}</math> for tension</p> <p>ELSEIF <math>\text{tr} \widehat{\mathbf{M}} &lt; 0</math> THEN</p> <p>apply <math>k_\vartheta(\vartheta)</math> and <math>\frac{\partial k_\vartheta(\vartheta)}{\partial \vartheta}</math> for compression</p> <p>ELSE</p> <math display="block">\widehat{\mathbf{C}}^{eg} = \widehat{\mathbf{C}}^e \quad \text{EXIT}</math> </li> <li>local Newton iteration           <ol style="list-style-type: none"> <li>compute residual               <math display="block">R_\vartheta = -\vartheta + \vartheta_n + \vartheta \Delta t</math> </li> <li>check tolerance               <p>IF <math>\ R_\vartheta\  &lt; \text{tol}</math> GOTO 4</p> </li> <li>compute incremental update               <math display="block">\Delta \vartheta = \overline{\partial_\vartheta \vartheta}^{-1} R_\vartheta</math> <p>with</p> <math display="block">\overline{\partial_\vartheta \vartheta} = 1 - \left[ \frac{\partial k_\vartheta}{\partial \vartheta} \text{tr} \widehat{\mathbf{M}} + k_\vartheta(\vartheta) \frac{\partial \text{tr} \widehat{\mathbf{M}}}{\partial \vartheta} \right] \Delta t</math> </li> <li>update               <math display="block">\vartheta \leftarrow \vartheta + \Delta \vartheta</math> <math display="block">\mathbf{F}_e = \frac{1}{\vartheta} \mathbf{F}; \quad \widehat{\mathbf{C}} = \mathbf{F}_e^t \cdot \mathbf{F}_e</math> <math display="block">\widehat{\mathbf{S}} = 2 \frac{\partial \psi_0}{\partial \widehat{\mathbf{C}}}; \quad \widehat{\mathbf{M}} = \widehat{\mathbf{C}} \cdot \widehat{\mathbf{S}}</math> </li> </ol> </li> <li>compute moduli           <math display="block">\widehat{\mathbf{C}}^{eg} = \widehat{\mathbf{C}}^e - \frac{2}{\vartheta} \overline{\partial_\vartheta \vartheta}^{-1} k_\vartheta(\vartheta) \Delta t</math> <math display="block">\left[ \widehat{\mathbf{C}}^e : \widehat{\mathbf{C}} \right] \otimes \left[ \widehat{\mathbf{S}} + \frac{1}{2} \widehat{\mathbf{C}} : \widehat{\mathbf{C}}^e \right]</math> <p>with <math>\widehat{\mathbf{C}}^e = 4 \frac{\partial^2 \psi_0}{\partial \widehat{\mathbf{C}}^2}</math></p> <p>and density</p> <math display="block">\rho_0 = \rho_0^* \vartheta^3</math> </li> </ol>
--

**Table 1** : Implicit Euler backward algorithm**Figure 12** : Deformation of the tube and evolution of the stretch ratio for an axial compression  $u = -0.5$ .**Figure 13** : Deformation of the inner boundary of the tube in radial direction.

tube, declining to the upper and lower boundary. The applied deformation is depicted in Fig. 13

for one cut along the axial direction through the tube. Herein the displayed deformation is chosen to  $u_r = 0.125$ . Fig. 14 shows the deformation and the evolution of the stretch ratio.

Herein we observe, that due to the stretch of the outside layer the material in the middle of the tube grows. At the upper and lower boundary atrophy is observed due to compression.

## 6 Conclusions

The main goal of this paper is the numerical implementation of a constitutive model for finite growth. In order to represent both a change in density and a change in volume, we applied a multiplicative split of the deformation gradient into a growth part and an elastic part. Consequently an additional presetting is required to describe the form of growth, this means the division of the total deformation into the elastic part and the growth part. We distinguish between different cases for a mass change, namely density preserving growth, volume pre-

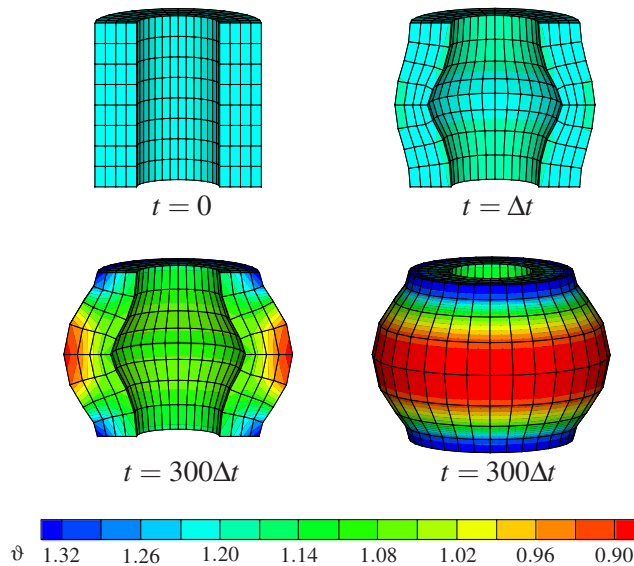


**Figure 14** : Deformation of the tube and evolution of the stretch ratio.

serving growth and growth in which both, the density and the volume, change. Since the volume preserving case has been studied intensively in earlier works, we focused in particular on the density preserving case. Changes in volume are characterised through the isotropic stretch ratio which is treated as an internal variable. In contrast to Lubarda & Hoger (2002), we assume the stretch ratio to be driven by the Mandel stresses  $\hat{\mathbf{M}}$  rather than by the elastic Piola-Kirchhoff stresses  $\hat{\mathbf{S}}$ . The constitutive equations have been implemented into a finite element code. Based on an implicit Euler backward scheme, the incremental tangent modulus as well as the algorithmic evolution of the stretch ratio have been derived. The theory has been discussed by numerical examples. At first the sensitivity of the material parameters has been shown by a simple tension test. Finally a cylindrical tube under homogeneous and an inhomogeneous deformation has been discussed within a finite element setting.

## References

**Ambrosi, D.; Mollica, F.** (2002): On the mechanics of a growing tumor. *International Journal of Engineering Science*, vol. 40, pp. 1297–1316.

**Beaupré, G. S.; Orr, T. E.; Carter, D. R.** (1990): An approach for time-dependent bone modeling and remodel-

ing - Theoretical development. *Journal of Orthopaedic Research*, vol. 8, pp. 651–661.

**Chen, Y.-C.; Hoger, A.** (2000): Constitutive functions of elastic materials in finite growth and deformation. *Journal of Elasticity*, vol. 59, pp. 175–193.

**Cowin, S. C.; Hegedus, D. H.** (1976): Bone remodeling i: Theory of adaptive elasticity. *Journal of Elasticity*, vol. 6, no. 3, pp. 313–326.

**Epstein, M.; Maugin, G. A.** (2000): Thermomechanics of volumetric growth in uniform bodies. *International Journal of Plasticity*, vol. 16, pp. 951–978.

**Garikipati, K.; Narayanan, H.; Arruda, E. M.; Grosh, K.; Calve, S.** (2004): Material forces in the context of biotissue remodelling. In Steinmann, P.; Maugin, G. A. (Eds): *Mechanics of Material Forces*, pp. 77–84. Euromech Colloquium 445. preprint.

**Harrigan, T. P.; Hamilton, J. J.** (1992): Optimality conditions for finite element simulation of adaptive bone remodeling. *International Journal of Solids and Structures*, vol. 29, no. 23, pp. 2897–2906.

**Harrigan, T. P.; Hamilton, J. J.** (1993): Finite element simulation of adaptive bone remodeling: A stability criterion and time stepping method. *International Journal for Numerical Methods in Engineering*, vol. 36, pp. 837–854.

**Himpel, G.** (2003): On the modeling of material growth in anisotropic solids. Internal variable approach and numerical implementation. Technical report, Institut für Mechanik (Bauwesen), Lehrstuhl I, Universität Stuttgart, Diplomarbeit, 2003. Report/Preprint No. 03-I-08.

**Holzappel, G. A.** (2000): *Nonlinear solid mechanics, a continuum approach for engineering*. Wiley.

**Holzappel, G. A.; Gasser, T. C.; Ogden, R. W.** (2000): A new constitutive framework for arterial wall mechanics and a comparative study of material models. *Journal of Elasticity*, vol. 61, pp. 1–48.

**Holzappel, G. A.; Ogden, R. W.** (Eds): *Biomechanics of soft tissue in cardiovascular systems*. No. 441 in CISM Courses and Lectures. Springer.

**Humphrey, J. D.** (2002): *Cardiovascular solid mechanics. Cells, tissues, and organs*. Springer.

- Humphrey, J. D.; Delange, S. L.** (2004): *An introduction to biomechanics*. Springer.
- Humphrey, J. D.; Rajagopal, K. R.** (2002): A constrained mixture model for growth and remodeling of soft tissues. *Mathematical Models and Methods in Applied Sciences*, vol. 12, pp. 407–430.
- Imatani, S.; Maugin, G. A.** (2002): A constitutive model for material growth and its application to three-dimensional finite element analysis. *Mechanics Research Communications*, vol. 29, pp. 477–483.
- Klisch, S. M.; van Dyke, T. J.; Hoger, A.** (2001): A theory of volumetric growth for compressible elastic biological materials. *Mathematics and Mechanics of Solids*, vol. 6, pp. 551–575.
- Kuhl, E.; Garikipati, K.; Arruda, E.; Grosh, K.** (2004): Remodeling of biological tissue: Mechanically induced reorientation of a transversely isotropic chain network. <http://arxiv.org/abs/q-bio.QM/0411037>. submitted for publication.
- Kuhl, E.; Menzel, A.; Garikipati, K.** (2004a): On the convexity of transversely isotropic chain network models. *Philosophical Magazine*. accepted for publication.
- Kuhl, E.; Menzel, A.; Steinmann, P.** (2003): Computational modeling of growth - A critical review, a classification of concepts and two new consistent approaches. *Computational Mechanics*, vol. 32, no. 1-2, pp. 71–88.
- Kuhl, E.; Steinmann, P.** (2003): Theory and numerics of geometrically nonlinear open system mechanics. *International Journal for Numerical Methods in Engineering*, vol. 58, pp. 1593–1615.
- Kuhl, E.; Steinmann, P.** (2003a): Mass- and volume specific views on thermodynamics for open systems. *Proceedings of the Royal Society of London A*, vol. 459, pp. 2547–2568.
- Kuhl, E.; Steinmann, P.** (2004): Computational modeling of healing: An application of the material force method. *Biomechanics and Modeling in Mechanobiology*, vol. 2, pp. 187–203.
- Lee, E. H.** (1969): Elastic-plastic deformation at finite strains. *Journal of Applied Mechanics*, vol. 36, pp. 1–6.
- Lubarda, V. A.** (2004): Constitutive theories based on the multiplicative decomposition of deformation gradient: Thermoelasticity, elastoplasticity, and biomechanics. *Applied Mechanics Reviews*, vol. 57, no. 2, pp. 95–108.
- Lubarda, V. A.; Hoger, A.** (2002): On the mechanics of solids with a growing mass. *International Journal of Solids and Structures*, vol. 39, pp. 4627–4664.
- Menzel, A.** (2005): Modelling of anisotropic growth in biological tissues - A new approach and computational aspects. *Biomechanics and Modeling in Mechanobiology*, vol. 3, no. 3, pp. 147–171.
- Menzel, A.** (2005a): Anisotropic remodelling of biological tissues. In Holzzapfel, G. A.; Ogden, R. W.(Eds): *IUTAM Symposium on Mechanics of Biological Tissue*. Springer. accepted for publication.
- Ogden, R. W.** (1997): *Non-linear elastic deformations*. Dover.
- Rao, I. J.; Humphrey, J. D.; Rajagopal, K. R.** (2003): Biological growth and remodeling: A uniaxial example with possible application to tendons and ligaments. *CMES: Computer Methods in Engineering and Sciences*, vol. 4, no. 3 & 4, pp. 439–455.
- Rodriguez, E. K.; Hoger, A.; McCulloch, A. D.** (1994): Stress-dependent finite growth in soft elastic tissues. *Journal of Biomechanics*, vol. 27, no. 4, pp. 455–467.
- Taber, L. A.** (1995): Biomechanics of growth, remodeling, and morphogenesis. *ASME Applied Mechanics Reviews*, vol. 48, no. 8, pp. 487–545.
- Taber, L. A.; Perucchio, R.** (2000): Modeling heart development. *Journal of Elasticity*, vol. 61, pp. 165–197.
- van Rietbergen, B.; Huiskes, R.; Eckstein, F.; Rügsegger, P.** (2003): Trabecular bone tissue strains in the healthy and osteoporotic human femur. *Journal of Bone and Mineral Research*, vol. 18, no. 10, pp. 1781–1788.